Journal of Molecular Structure 1087 (2015) 80–87

Contents lists available at ScienceDirect

Journal of Molecular Structure

journal homepage: www.elsevier.com/locate/molstruc

Crystal structure, spectroscopic and thermal properties of $[Zn(Lap)_2(DMF)(H_2O)]$ and isomorphous $[M(Lap)_2]_n$ (M: Cd, Mn) complexes

R.A. Farfán [a,*], J.A. Espíndola [a], M.I. Gomez [b], M.C.L. de Jiménez [b], O.E. Piro [c], E.E. Castellano [d], M.A. Martínez [b]

[a] Facultad de Ciencias Exactas, Universidad Nacional de Salta, Avda. Bolivia 5150, 4400 Salta, Argentina
[b] Facultad de Bioquímica, Química y Farmacia, Universidad Nacional de Tucumán, Ayacucho 471, 4000 Tucumán, Argentina
[c] Departamento de Física, Facultad de Ciencias Exactas, Universidad Nacional de La Plata and Institute IFLP (CONICET, CCT-La Plata), C.C. 67, 1900 La Plata, Argentina
[d] Instituto de Física de São Carlos, Universidade de São Paulo, C.P. 369, 13560 São Carlos, SP, Brazil

HIGHLIGHTS

- A new series of lapachol complexes with Zn, Cd and Mn ions were synthesized.
- The solid state structures of the compounds were determined by X-ray diffraction.
- The vibration, electronic, and thermal behavior of the substances are presented.

ARTICLE INFO

Article history:
Received 30 September 2014
Received in revised form 24 December 2014
Accepted 23 January 2015
Available online 31 January 2015

Keywords:
Lapacholate
Zn(II)
Cd(II) and Mn(II) complexes
Crystal structures
Spectroscopic properties

ABSTRACT

The solid state structure of the lapacholate (Lap^-) complexes with Zn(II), Cd(II) and Mn(II) were determined by X-ray diffraction methods. $[Zn(Lap)_2(DMF)(H_2O)]$ crystallizes in the triclinic space group $P\bar{1}$ with $a = 10.5051(4)$, $b = 12.8020(4)$, $c = 13.0394(4)$ Å, $\alpha = 60.418(2)$, $\beta = 83.904(2)$, $\gamma = 86.206(2)°$, and $Z = 2$ molecules per unit cell. The isomorphous complexes $[M(Lap)_2]_n$ (M: Cd, Mn) crystallize in the tetragonal space group $P4_32_12$ with $a = b = 13.5770(6)$ Å, $c = 14.5730(6)$ Å (Cd), and $a = b = 13.3539(4)$, $c = 14.7148(4)$ Å (Mn), and $Z = 4$. In $[Zn(Lap)_2(DMF)(H_2O)]$ the Zn(II) ion is in a distorted octahedral environment coordinated to two different and nearly perpendicular Lap^- molecules acting as bidentate ligands through their adjacent carbonyl and phenol oxygen atoms. The remaining two *cis*-coordination sites are occupied by water and DMF molecules. $[M(Lap)_2]_n$ (M: Cd, Mn) isomorphous complexes are also octahedral and present a supra-molecular arrangement in the lattice. There is only one independent Lap^- molecule that coordinates the metal through all three ligand binding sites, giving rise to a 3-D structure of $[M(Lap)_2]_n$ complexes that extends throughout the crystal lattice.

The lapachol binding to metal is also revealed by the IR spectra. In fact, the carbonyl C=O stretching frequency is appreciable red-shifted in the complexes as compared to uncoordinated lapachol ligand. As expected, the IR and UV–Vis spectra of the isomorphous pair of complexes closely resemble to each other.

Up to above 300 °C there are significant differences in the TGA of the Zn complex when compared with the isomorphous pair: while the former shows the loss of the secondary ligands (water and DMF), the latter exhibits a plateau signaling the lesser labile character of the lapacholate ligand.

Introduction

Lapachol (HLap), a natural product that can be extracted from the wood of lapacho tree (gendre *Tabebuia Ipé*), and their derivatives are employed as anti-tumor, antibiotic, antimalaria and anti-ulcer pharmaceuticals [1,2]. Besides, lapachol is also considered as probable anti-cancer agent [3] and with potential to fight the *trypanosomacruzi*, the protozoo causing the Chagas' disease [4]. Lapachol is structurally a naphthoquinone with an unsaturated pendant chain at the C3-position and an oxydryl group at the C2-position, being described as [2-hydroxy-3-(3-methyl-2-butenyl)-1,4-naphthoquinone] [4]. In an alkaline

* Corresponding author.

http://dx.doi.org/10.1016/j.molstruc.2015.01.042
0022-2860/

medium, the lapachol loses the oxydryl proton and turns into a potential bidentate ligand (Lap^-) with the ability to bind divalent metal ions.

Lapacholate molecule constitutes a versatile ligand for metal ion coordination as it presents three binding sites, namely the unprotonated phenol and the two carbonyl oxygen atoms, with the phenol and the adjacent carbonyl oxygen atoms usually acting as a 'bite' to bind the metal.

Previously we reported the molecular structures of $Zn(Lap)_2(EtOH)_2$ and $Co(Lap)_2(DMF)(H_2O)$ complexes [5,6]. In the zinc complex, the metal is located at a crystallographic inversion center in an octahedral environment, equatorially *trans*-coordinated to two symmetry related Lap^- molecules acting as bidentate ligand through the phenol and the adjacent carbonyl oxygen atoms. The metal is axially coordinated to the oxygen atom of two EtOH molecules. The cobalt octahedral complex is also coordinated to two Lap^- anions but now with their coordination planes nearly perpendicular to each other. The remaining binding sites are occupied by DMF and water molecules.

Recently, we synthesized and solved the molecular structure of the Ni(II) complex, $Ni(Lap)_2(DMF)(H_2O)$ [7]. In this complex, the nickel ion is in an octahedral coordination but now equatorially *cis*-coordinated to two Lap^- ligands. The metal is axially coordinated to DMF and water molecules.

We report here the crystal structure of $Zn(Lap)_2(DMF)(H_2O)$ and isomorphous $[M(Lap)_2]_n$ (M: Cd, Mn) complexes. The zinc complex is isomorphous to $Co(Lap)_2(DMF)(H_2O)$ [6]. The manganese complex is the chiral counterpart of the $[Mn(Lap)_2]_n$ structure reported by Caruso et al. [8]. In the cadmium(II) and manganese(II) complexes, the metal ion is also coordinated to two Lap^- anions (here, symmetry related) acting as bidentate ligands in a binding mode closely related to the zinc complex, but now it presents the novelty that the remaining binding sites are occupied by the other carbonyl oxygen atom of two, also symmetry related, Lap^- molecules, giving rise to a 3-D net of metal complexes in the crystal lattice.

Experimental

Methods

Vibrational spectra

Infrared spectra (in the 4000–400 cm^{-1} region) were recorded at room temperature (RT) on a FTIR Perkin Elmer GX FTIR working in the transmission mode and using KBr pellets.

The electronic spectra (UV–Vis) of both solutions of DMF samples were run on a double-beam GBC 918 spectrophotometer.

Thermo-gravimetric analysis (TGA)

TGA was performed with a Shimadzu TGA-50 instrument under flowing oxygen (50 mL/min) at a heating rate of 5 °C/min from room temperature up to 500 °C.

X-ray diffraction data

The measurements were performed on an Enraf–Nonius Kappa-CCD diffractometer with graphite-monochromated Mo Kα (λ = 0.71073 Å) radiation. Diffraction data were collected (φ and ω scans with κ-offsets) with COLLECT [9]. Integration and scaling of the reflections was performed with the HKL DENZO-SCALEPACK [10] suite of programs. The unit cell parameters were obtained by least-squares refinement based on the angular settings for all collected reflections using HKL SCALEPACK [10]. The data were corrected numerically for absorption with PLATON [11]. The structures were solved by direct methods with SHELXS-97 of the SHELX [12] suite of programs and the corresponding molecular models developed by alternated cycles of Fourier methods and full-matrix least-squares refinement with SHELXL-97 of the same package. The hydrogen atoms of the lapacholate anion were positioned stereo-chemically and refined with the riding model. The methyl hydrogen atoms locations were optimized during the refinement by treating them as rigid bodies which were allowed to rotate around the corresponding C—CH_3 bond such as to maximize the residual electron density at the calculated positions. The water H-atoms of $Zn(Lap)_2(DMF)(H_2O)$ were located in a difference Fourier map and refined at their found positions with an isotropic displacement parameter 50% larger than the one of the water oxygen. Crystal data and refinement results are summarized in Table 1.

Synthesis

$Zn(Lap)_2(DMF)(H_2O)$

Two solutions were prepared: one of them by diluting 1.22 g of HLap in 100 mL of methanol, the other one by diluting 0.7 g of $Zn(CH_3COO)_2{\cdot}2H_2O$ in 100 mL of water. Both solutions were heated up to of 65 °C before mixing them under magnetic stirring. This resulted in a characteristic dark-red solid deposition which was then filtered out from the solution and washed with abundant water to eliminate uncoordinated metal ions before allowing it to dry. The resulting solid was completely dissolved in DMF and single crystals adequate for structural X-ray diffraction studies were obtained by slow evaporation of the solvent (yield of 61.53%).

$[M(Lap)_2]_n$ (M: Mn, Cd)

0.26 g of $Mn(CH_3COO)_2$ were dissolved in 50 mL of water and 0.75 g of lapachol was dissolved in 50 mL of ethanol. Both solutions were mixed and heated up to 65 °C under continuous stirring. After half an hour it was observed the deposition of the characteristic dark-red solid. The solution was left to cool down to room temperature and then the solid was filtered out from the solution and washed with abundant water to eliminate uncoordinated Mn(II) ions. The obtained solid was then dried in a vacuum desiccator. A portion of the resulting material was completely dissolved in DMF and the solvent allowed to slowly evaporate until the appearance of single crystals appropriate for structural X-ray diffraction work (yield of 62.02%). An entirely similar procedure starting with 0.43 g of $Cd(CH_3COO)_2$ afforded the synthesis of adequate $Cd(Lap)_2$ single crystals (yield of 65.21%).

Results and discussion

Structural X-ray diffraction

ORTEP [13] drawings of $[Zn(Lap)_2(DMF)(H_2O)]$ and $[Cd(Lap)_2]_n$ complexes are shown in Figs. 1 and 2. Corresponding bond distances and angles around the metal ion in the zinc complex and the isomorphous cadmium and manganese compounds are in Tables 2 and 3, respectively.

$[Zn(Lap)_2(DMF)(H_2O)]$

The complex is isomorphous to $Co(Lap)_2(DMF)(H_2O)$ [6]. In fact, the *rms* separation between homologous non-H atoms in the best least-squares structural fitting of the Zn and Co complexes, calculated by the Kabsh's procedure [14], is 0.061 Å. The Zn(II) ion is in a distorted octahedral environment coordinated to two nearly perpendicular and different lapacholate anions acting as bidentate ligands through their adjacent carbonyl and phenol oxygen atoms [Zn—O bond distances of 2.139(2) and 2.044(2) Å for ligand 1 and 2.141(2) and 2.071(2) Å for ligand 2, respectively]. The other *cis*-positions around the metal are occupied by water [d(Zn—Ow) = 2.104(2) Å] and DMF [d(Zn—O) = 2.105(2) Å] mole-

Table 1
Crystal data and structure refinement for $[Zn(Lap)_2(DMF)(H_2O)]$ and isomorphous $[M(Lap)_2]_n$ (M: Cd, Mn) complexes.

Compound	$[Zn(Lap)_2(DMF)(H_2O)]$	$[Cd(Lap)_2]_n$	$[Mn(Lap)_2]_n$
Empirical formula	$C_{33}H_{35}NO_8Zn$	$C_{30}H_{26}CdO_6$	$C_{30}H_{26}MnO_6$
Formula weight	638.99	594.91	537.45
Temperature (K)	296(2)	296(2)	296(2)
Wavelength (Å)	0.71073	0.71073	0.71073
Crystal system	Triclinic	Tetragonal	Tetragonal
Space group	$P\bar{1}$	$P4_32_12$	$P4_32_12$
Unit cell dimensions			
a (Å)	10.5051(4)	13.5770(6)	13.3539(4)
b (Å)	12.8020(4)	13.5770(6)	13.3539(4)
c (Å)	13.0394(4)	14.5730(6)	14.7148(4)
α (°)	60.418(2)		
β (°)	83.904(2)		
γ (°)	86.206(2)		
Volume (Å^3)	1516.22(9)	2686.3(2)	2624.0(1)
Z, density (calc., Mg/m^3)	2, 1.400	4, 1.471	4, 1.360
Absorption coefficient (mm^{-1})	0.863	0.850	0.545
$F(000)$	668	1208	1116
Crystal size (mm^3)	0.350 × 0.262 × 0.049	0.205 × 0.154 × 0.120	0.290 × 0.279 × 0.272
Crystal color/shape	Dark red/fragment	Dark red/prism	Dark red/polyhedral
ϑ-range (°) for data collection	2.70–26.00	3.00–25.68	2.56–25.97
Index ranges	$-12 \leqslant h \leqslant 12$, $-15 \leqslant k \leqslant 15$, $-16 \leqslant l \leqslant 16$	$-9 \leqslant h \leqslant 16$, $-16 \leqslant k \leqslant 16$, $-17 \leqslant l \leqslant 16$	$-11 \leqslant h \leqslant 16$, $-15 \leqslant k \leqslant 16$, $-18 \leqslant l \leqslant 17$
Reflections collected	16882	8246	8994
Independent reflections	5889 [R(int) = 0.0855]	2553 [R(int) = 0.0338]	2579 [R(int) = 0.0394]
Observed reflections [$I > 2\sigma(I)$]	4984	2252	2330
Completeness (%)	99.1 (to ϑ = 26.00°)	99.7 (to ϑ = 25.68°)	99.7 (to ϑ = 25.97°)
Refinement method	Full-matrix least-squares on F^2	Full-matrix least-squares on F^2	Full-matrix least-squares on F^2
Data/restraints/parameters	5889/0/394	2553/0/170	2579/0/171
Goodness-of-fit on F^2	1.051	1.087	1.084
Final R indices[a] [$I > 2\sigma(I)$]	R_1 = 0.0451, wR_2 = 0.1140	R_1 = 0.0315, wR_2 = 0.0795	R_1 = 0.0333, wR_2 = 0.0834
R indices (all data)	R_1 = 0.0554, wR_2 = 0.1220	R_1 = 0.0400, wR_2 = 0.0854	R_1 = 0.0408, wR_2 = 0.0884
Absolute structure parameter		−0.06(4)	−0.02(2)
Larg. diff. peak and hole (e Å^{-3})	0.623 and −0.958	0.401 and −0.445	0.237 and −0.355

[a] $R_1 = \Sigma||F_o| - |F_c||/\Sigma|F_o|$, $wR_2 = [\Sigma w(|F_o|^2 - |F_c|^2)^2/\Sigma w(|F_o|^2)^2]^{1/2}$.

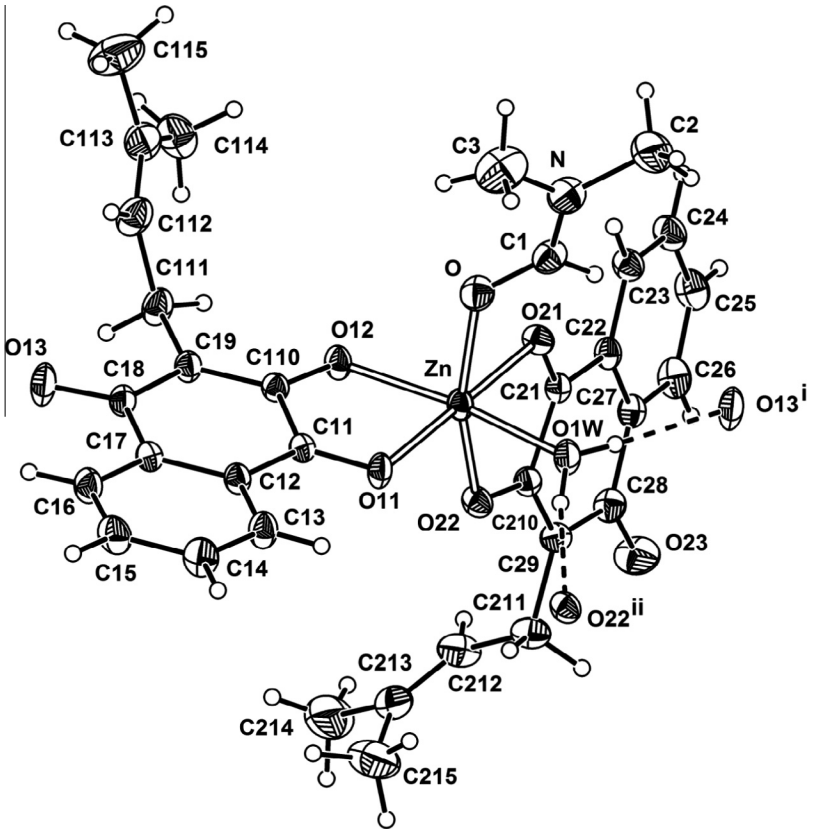

Fig. 1. Plot of the $[Zn(Lap)_2(DMF)(H_2O)]$ complex showing the labeling of the non-H atoms and their displacement ellipsoids at the 30% probability level. Metal–ligand bonds are indicated by open bonds and intermolecular H-bonds by dashed lines. Symmetry operations are: (i) $x + 1/2, y, z$; (ii) $-x + 1, -y + 2, -z$.

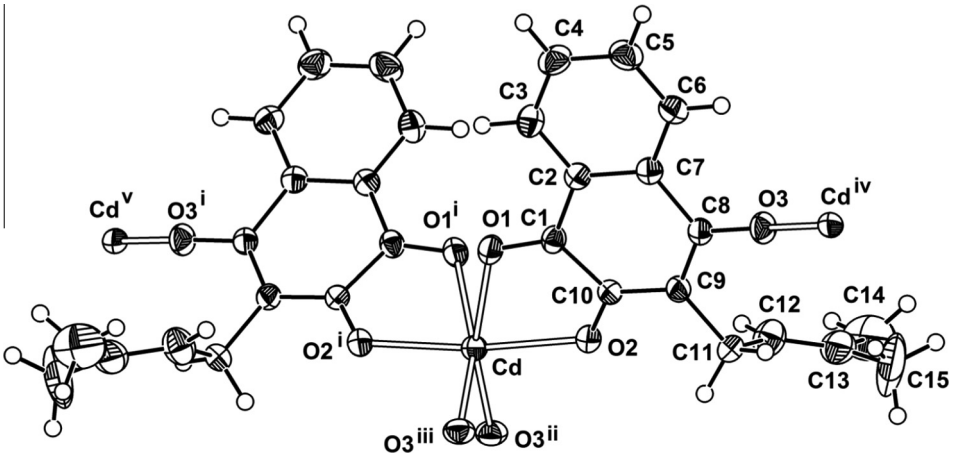

Fig. 2. Drawing of the $[Cd(Lap)_2]_n$ complex. The view includes two symmetry related Cd(II) ions to show the arrangement of cadmium complexes extending throughout the crystal lattice. Symmetry operations are: (i) $-y, -x, -z + 1/2$; (ii) $y - 1/2, -x + 1/2, z + 1/4$; (iii) $x - 1/2, -y + 1/2, -z + 1/4$; (iv) $-y + 1/2, x + 1/2, z - 1/4$; (v) $-x - 1/2, y - 1/2, -z + 3/4$.

Table 2
Bond lengths (Å) and angles (°) around Zn(II) ion in $[Zn(Lap)_2(DMF)(H_2O)]$.

Zn—O(12)	2.044(2)	O(22)—Zn—O	163.65(7)
Zn—O(22)	2.071(2)	O(1W)—Zn—O	85.45(8)
Zn—O(1W)	2.104(2)	O(12)—Zn—O(11)	78.15(6)
Zn—O	2.105(2)	O(22)—Zn—O(11)	101.05(7)
Zn—O(11)	2.139(2)	O(1W)—Zn—O(11)	85.87(7)
Zn—O(21)	2.141(2)	O—Zn—O(11)	93.77(8)
		O(12)—Zn—O(21)	100.49(7)
O(12)—Zn—O(22)	99.30(7)	O(22)—Zn—O(21)	77.65(6)
O(12)—Zn—O(1W)	163.20(7)	O(1W)—Zn—O(21)	95.61(7)
O(22)—Zn—O(1W)	88.75(7)	O—Zn—O(21)	87.71(7)
O(12)—Zn—O	90.40(7)	O(11)—Zn—O(21)	177.98(6)

Table 3
Bond lengths (Å) and angles (°) around M(II) ion in $[M(Lap)_2]_n$ (M: Cd, Mn).

$[Cd(Lap)_2]_n$		$[Mn(Lap)_2]_n$	
Cd—O(2)	2.179(2)	Mn—O(2)	2.108(1)
Cd—O(3)#2	2.246(2)	Mn—O(3)#2	2.114(1)
Cd—O(1)	2.377(3)	Mn—O(1)	2.319(2)
O(2)—Cd—O(2)#1	172.7(1)	O(2)—Mn—O(2)#1	169.18(8)
O(2)—Cd—O(3)#2	92.8(1)	O(2)—Mn—O(3)#2	93.05(7)
O(2)—Cd—O(3)#3	92.3(1)	O(2)—Mn—O(3)#3	94.36(7)
O(3)#2—Cd—O(3)#3	91.3(1)	O(3)#2—Mn—O(3)#3	93.44(8)
O(2)—Cd—O(1)	72.16(9)	O(2)—Mn—O(1)	73.41(6)
O(2)#1—Cd—O(1)	102.09(9)	O(2)#1—Mn—O(1)	98.06(6)
O(3)#2—Cd—O(1)	163.4(1)	O(3)#2—Mn—O(1)	164.32(6)
O(3)#3—Cd—O(1)	96.2(1)	O(3)#3—Mn—O(1)	95.41(6)
O(1)—Cd—O(1)#1	80.6(1)	O(1)—Mn—O(1)#1	79.11(9)

Symmetry transformations used to generate equivalent atoms: (#1) $-y, -x, -z + 1/2$; (#2) $y - 1/2, -x + 1/2, z + 1/4$; (#3) $x - 1/2, -y + 1/2, -z + 1/4$.

cules. *Trans* O—Zn—O angles in the ZnO_6 core are in the range from 163.20(7)° to 177.98(6)° and *cis* O—Zn—O angles are within the 77.65(6)–101.05(7)° interval. Both lapacholate ligands are planar (*rms* deviation of fitted atoms from the least-squares plane is 0.054 Å for lapacholate 1 and 0.089 Å for lapacholate 2) and nearly perpendicular to each other [angled in 75.96(4)°] with the Zn(II) ion laying close onto the planes intersection [at less than 0.091(2) Å].

The coordination water molecule bridges two neighboring complexes in the lattice through Ow—H···O bonds (see Fig. 1), one with unbonded-to-metal carbonyl oxygen [$d(H\cdots O13^{i}) = 1.933$ Å, $\angle(Ow—H\cdots O13^{i}) = 176.9°$], the other one with a phenol oxygen [$d(H\cdots O22^{ii}) = 1.941$ Å, $\angle(Ow—H\cdots O) = 170.4°$]. Further details of the H-bonding structure are given in Table 4.

$[M(Lap)_2]_n$ (M: Cd, Mn)

The complexes are isomorphous to each other. The *rms* separation between homologous non-H atoms in the best least-squares structural fitting of the complexes is 0.055 Å. In these highly symmetric tetragonal crystals, there is only one independent lapacholate ligand employing all three binding sites to coordinate the M(II) ions. In fact the metal is sited on a crystallographic twofold axis in a distorted octahedral environment bound to four symmetry-related Lap^- ligands, two of them with a binding mode that resembles the one described above for the zinc complex [M—O_{carb} and M—O_{ph} bond distances of 2.377(3) and 2.179(2) Å for the Cd complex and 2.319(2) and 2.106(1) Å for the Mn one], the other two occupying the remaining binding *cis*-positions through their other, *para* carbonyl, oxygen atoms [$d(Cd—O_{carb}) = 2.246(2)$ Å and $d(Mn—O_{carb}) = 2.114(1)$ Å]. The slightly longer Cd—O bonds as compared with the corresponding Mn—O ones reflect the larger Cd(II) ionic radii (0.97 Å) as compared with Mn(II) radii (0.80 Å). This metal coordination gives rise to a supra-molecular structure of metal complexes in the crystal lattice (see Fig. 2). *Trans* O—M—O angles in the MO_6 core are in the 163.4(1)–172.7(1)° range for the Cd complex and within the 164.32(6)–169.18(2)° interval for the Mn one, and *cis* O—M—O angles are in the 72.15(9)–102.09(9)° range (Cd) and within the 73.41(6)–98.06(6)° interval (Mn).

The Lap ligand is nearly planar (*rms* deviation of fitted atoms from the least-squares plane are 0.129 and 0.141 Å for the Cd and Mn complexes) with the metal ion laying close onto the corresponding plane [at 0.064(3) and 0.015(2) Å].

Interestingly, our $[Mn(Lap)_2]_n$ crystal [space group $P4_32_12$, Flack's absolute structure parameter [15] equal to −0.02(2)] is the chiral counterpart of the corresponding manganese complex [8] [space group $P4_12_12$, Flack's parameter = 0.004(16)]. The Flack's parameter is the fractional contribution to the diffraction pattern due to the molecule's racemic twin and for the correct enantiomorphous crystal it should be zero to within experimental error [12]. This suggests that the $[Mn(Lap)_2]_n$ crystal samples could be racemic conglomerates generated by spontaneous resolution, a rare event discovered by L. Pasteur in 1848 to occurs in the crystallization of racemic sodium ammonium tartrate tetrahydrate from aqueous solution [16–18].

Chemical analysis and properties of the complexes

The color of the crystals varies from dark red to brown, in contrast with both the yellow color of uncoordinated lapachol

Table 4
Hydrogen bond distances (Å) and angles (°) in $Zn(Lap)_2(DMF)(H_2O)$.

D—H	d(D—H)	d(H···A)	∠DHA	d(D···A)	A	Symmetry operation
O1W—H1W	0.804	1.933	176.91	2.736	O13	[x + 1, y, z]
O1W—H2W	0.836	1.941	170.43	2.769	O22	[−x + 1, −y + 2, −z]

(pK_a = 6.15) and the red appearance of sodium lapacholate. The complexes are very stable at ambient conditions and their solubility in a few common solvents is shown in Tables 5 and 4. Though the complexes dissolve rapidly in DMF, this solvent presents the ability to bind to metal ions and thus it could enter the metal coordination sphere as a secondary ligand competing with ethanol, methanol or water molecules, as in the case of the Zn complex [5].

The lapachol content of the complexes were determined by the methodology reported by Martínez *et al.*, namely by measuring the absorbance of the various solutions at wavelengths of 330 nm and 390 nm, the spectral regions where the lapachol ligand exhibits its absorption maxima ($\varepsilon_{330} = 2.8 \times 10^3\ cm^{-1}\ M^{-1}$ and $\varepsilon_{390} = 1.4 \times 10^3\ cm^{-1}\ M^{-1}$) [5,6]. With this data and the known solution concentration it is possible to find the percentage of lapachol in the different coordination compound through the Beer's Law. These percentages were determined from atomic absorption spectrophotometry (AAS) measurements and the results are shown in Table 6 where they are compared with the theoretically expected values.

Thermo-gravimetric analysis

The thermo-gravimetric behavior of the Zn, Cd and Mn complexes are shown in Fig. 3. The Zn thermo-gravimetric curve (Fig. 3a) shows up to 290 °C a mass loss of 14.08% that corresponds to the water and DMF elimination (theoretical value of 14.24%). The total mass loss percentage is 87.11%, in agreement with the theoretical loss (87.58%) calculated for the formation of ZnO from the complex.

It can be appreciated in the Cd and Mn compounds (see Fig. 3) the presence of wide plateaus, a signature for the absence of secondary ligands (which are expected to be more labile than the lapachol ligand). The decomposition onset temperature is observed at 290 °C for the Cd compound and 311 °C for Mn and indicates the starting of oxidative reactions which in turn proceed in steps. The mass loss percentages are 78.0% and 85.95% for the Cd and Mn complexes, respectively. These values are in agreement with the theoretical losses (78.42% and 85.31%) calculated for the formation of CdO and Mn_2O_3 oxides from the complexes.

Vibrational spectroscopy

$Zn(Lap)_2(DMF)(H_2O)$

Fig. 4 shows the IR absorption spectrum of the Zn complex. In the O—H stretching region it is observed a broad band centered at about 3338 cm^{-1} probably due to atmospheric water and around 3270(II) cm^{-1} it can be appreciated a shoulder that can be explained as due to H-bonded O—H stretch. In the 2800–3000 cm^{-1} spectral range there appear bands due to CH—CH, CH_2 and CH_3 stretching modes.

Table 6
Spectrophotometric chemical analysis of the Zn, Cd and Mn complexes.

Complex	%	% HLap	% M
$Zn(Lap)_2(DMF)(H_2O)$	Expected	75.82	10.23
	Experim.	76.20	10.43
$[Cd(Lap)_2]_n$	Expected	81.44	18.89
	Experim.	82.90	19.21
$[Mn(Lap)_2]_n$	Expected	89.78	10.22
	Experim.	88.86	10.04

The C=O stretching bands of the quinone groups coordinated to the metal, namely the C_{11}=O_{11} and C_{21}=O_{21} groups, are observed at 1632 cm^{-1}, considerably red-shifted as compared with the corresponding frequency of uncoordinated lapachol (1662 cm^{-1}) [8]. The corresponding stretching bands of the non coordinated-to-metal C_{18}=O_{13} and C_{28}=O_{23} groups are observed around 1587 cm^{-1}, significantly red-shifted as compared with lapachol (1641 cm^{-1}), a fact clearly related to the strong O···H—O_w interaction of both groups with the water molecule as revealed by the structural X-ray study. All these bands are red-shifted when compared with the lapachol corresponding ones (detected as groups centered around 1661 and 1639 cm^{-1}). The above mentioned frequency shifts are also affected by resonance operating between the *p*-and *o*-naftoquinone forms which involves both coordinated and non-coordinated carbonyl groups.

The intense and sharp IR absorption band at 1666 cm^{-1} is attributed to DMF ν(C=O) mode [6]. This band shifts to lower frequency with respect to un-bonded DMF (1678 cm^{-1}) due to coordination of DMF oxygen to the metal, as disclosed from the structural X-ray results [19].

The intense and sharp band at 1535 cm^{-1} is assigned to a stretching C—C mode of the quinoline rings. The IR band observed at 1364 cm^{-1} is assigned to the DMF C—N stretch, within the reported range for this mode (1370–1350 cm^{-1}). It is to be noted that in amides, where the carbonyl group is part of a conjugated system, there are three atoms involved in the electronic rearrangement upon coordination which leads to frequency shifts as compared with un-bonded DMF [20]. For a tentative assignment of C=O stretching mode of phenolic carbonyl groups (namely, $C_{110}O_{12}$ and $C_{210}O_{22}$ of Fig. 1) we shall refer to spectroscopic data of related complexes and to the assistance of Quantum Chemical calculations on the Ni(II) lapacholate [7]. These predict a ν(C=O) frequency of 1306 cm^{-1}, being the nearest bands observed in the 1296–1240 cm^{-1} range. This is in agreement with that reported in previous studies [7]. The sharp band observed at 736 cm^{-1} is assigned to an out-of-plane ring mode combined with C—C—H deformations as suggested by the calculations and the results

Table 5
Solubility of $Zn(Lap)_2(DMF)(H_2O)$ and $[M(Lap)_2]_n$ (M: Cd, Mn) complexes.

	ETOH	MeOH	Benzene	Acetone	Ether	DMF	H_2O
$[Zn(Lap)_2(DMF)(H_2O)]$	sl	s	i	sl	sl	vs	i
$[Cd(Lap)_2]$	s	s	s	s	sl	vs	i
$[Mn(Lap)_2]$	sl	sl	i	i	i	vs	i

sl: slightly soluble, s: soluble, vs: very soluble, i: insoluble.

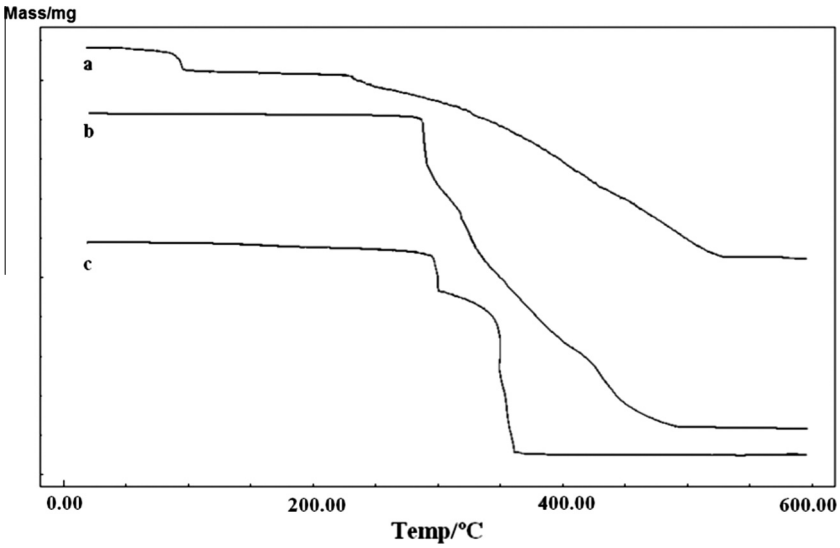

Fig. 3. Thermo-gravimetric curves of: (a) $Zn(Lap)_2(DMF)(H_2O)$, (b) $[Cd(Lap)_2]_n$, and (c) $[Mn(Lap)_2]_n$.

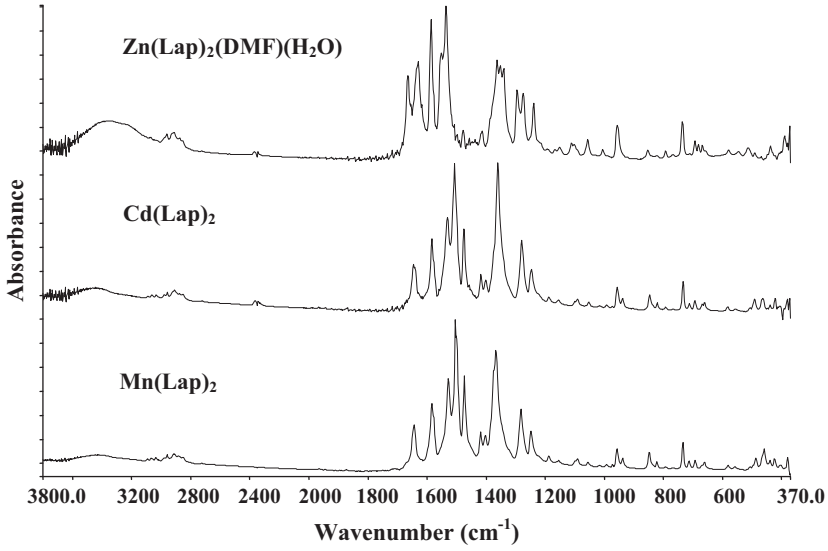

Fig. 4. IR absorption spectra of $Zn(Lap)_2(DMF)(H_2O)$ and isomorphous $[M(Lap)_2]_n$ (M: Cd, Mn) complexes.

reported by Bustamante et al. [23]. In the low-frequency region are observed IR bands at 439, 391 and 374 cm^{-1} which (within the spectral range limitation of the spectrophotometer) could be attributed to M—O stretching modes [22].

$M(Lap)_2$ (M: Mn, Cd)

As expected from the crystallographic results revealing their mutual isomorphism, the absorption IR spectra of the compounds are nearly identical with minor differences observed in the low-frequency region (see Fig. 4).

The low-intensity and broad band observed at 3448 cm^{-1} is attributed to humidity of the sample holder. In this region does not appear the intense and sharp band due to lapachol OH stretching mode (at 3352 cm^{-1}) because lapachol is deprotonated to coordinate with the metal ion. The bands located within the 3100–2850 cm^{-1} spectral range are assigned to C—H stretching modes of aliphatic and aromatic groups in both complexes.

In the C=O stretching region of the coordinated carbonyl groups are is observed the characteristic bands at 1645 and 1585 cm^{-1} (Mn) and at 1647 and 1585 cm^{-1} (Cd) showing the typical frequency red shift as compared with the corresponding bands of lapachol (1661 and 1639 cm^{-1}) due to coordination to the metal.

A new series of intense and sharp bands are observed at 1528, 1510 and 1475 cm^{-1} (Mn) and at 1532, 1515 and 1476 cm^{-1} (Cd) which can be assigned to C=C—C stretching and C—H deformation modes.

The intense and sharp band observed at 1368 cm^{-1} in the IR of the complexes appears at the same spectral position as in pure lapachol where it is assigned to a C—H scissor mode of the lateral group.

In the 1283–1249 cm^{-1} (Mn) and 1281–1248 cm^{-1} (Cd) spectral ranges are observed two medium intensity and sharp bands which are attributed to C—C and phenol C—O stretching modes, and to C—H and phenol C—O stretching modes [24,25].

The IR band found at 735 cm^{-1} appears blue-shifted when compared with the corresponding one of lapachol (at 724 cm^{-1}) where it is assigned to out-of-plane ring modes combined with torsion H—C—C—C modes. The presence of various vibration modes in this region makes it difficult a detailed assignment of spectral features.

The weak absorption bands below about 500 cm^{-1} could be assigned to metal–ligand modes and they show up at 488, 459, 441, 426, and 381 cm^{-1} (Mn) and at 488, 464, 422 and 382 cm^{-1} (Cd) [21,22].

Electron spectroscopy

The electronic absorption spectra in the UV–visible region of the Zn(II), Cd(II) and Mn(II) coordination compounds were obtained from a mixed DMF-H_2O 10^{-5} M solution and turned out to be quite similar to one another, as shown in Fig. 5.

For the Zn complex it is observed a shoulder at 330 nm and a very broad absorption band in the visible centered around 505 nm. This band can be assigned to a $n \rightarrow \pi^*$ transition involving the quinolinic carbonyl groups. The band at 277 nm (quinolinic ring) and the shoulder at 330 nm (benzene ring) can be assigned to aromatic ring $\pi \rightarrow \pi^*$ transitions [26,27].

As expected, the spectra of isomorphous Cd and Mn complexes closely resemble to each other. They show a weak shoulder at about 295 nm, and another, more pronounced, at 330 nm (Cd) and 340 nm (Mn), attributable to $\pi \rightarrow \pi^*$ transitions, and a very broad band centered around 500 nm (Cd) and 505 nm (Mn), which gives rise to the characteristic color of the lapachol complexes [8].

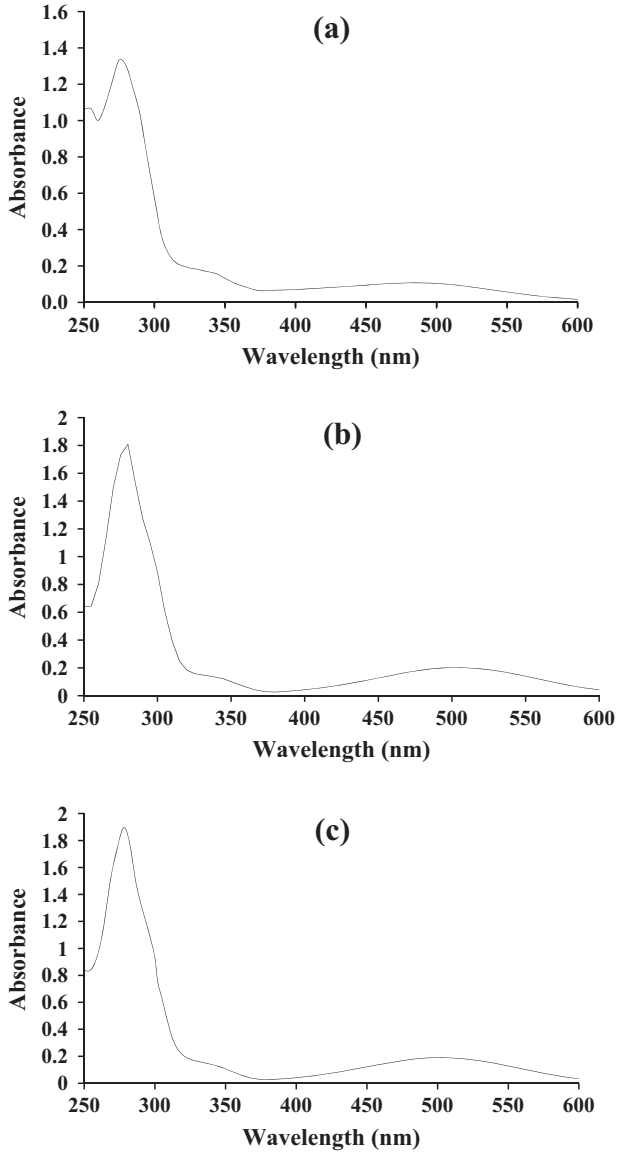

Fig. 5. Electron absorption spectra: (a) $Zn(Lap)_2(DMF)(H_2O)$, (b) $[Cd(Lap)_2]_n$, and (c) $[Mn(Lap)_2]_n$.

Conclusions

Three new complexes of Zn, Cd and Mn were synthesized with lapachol as main ligand and we report here the crystal structure of $Zn(Lap)_2(DMF)(H_2O)$ and isomorphous $[M(Lap)_2]_n$ (M: Cd, Mn) as further members of an ever growing family of lapacholate-metal complexes. Although both water and DMF are involved in the synthesis of the three compounds, only in the Zn complex these molecules are coordinated to the metal ion as secondary ligands. The Zn thermo-gravimetric curve shows up to 290 °C a mass loss that corresponds to elimination of water and DMF. In contrast, for the Cd and Mn compounds it was observed wide plateaus that extend up to above 300 °C which indicate the absence of labile ligands.

The metal ions act as acceptors of electrons donated by carbonyl and phenolic oxygen atoms in position 1 and 2 of the lapacholate naphthoquinone ring. This gives rise to CTLM transitions detected in the visible spectra as broad and strong absorption bands centered at 505 nm (Zn), 500 nm (Cd) and 505 nm (Mn). These absorptions are the origin of the intense red-brown color exhibited by the complexes and can be attributed to p-quinone ↔ o-quinone mesomerism in the quinonic ring conjugated system.

$[Mn(Lap)_2]_n$ complex (space group $P4_32_12$) can also crystallize as its chiral counterpart (SG $P4_12_12$). This suggests that the manganese complex could be an uncommon example of substances whose crystallization produces racemic conglomerates generated by spontaneous resolution.

Acknowledgments

This work was supported by CONICET of Argentina and FAPESP of Brazil. O.E.P is a Research Fellow of CONICET. M.I.G. thanks to CIUNT (Project 26D-517) and R.A.F and J.A.E. thank to CIUNS of Argentina for financial support.

Appendix A. Supplementary material

Listings of fractional coordinates and equivalent isotropic displacement parameters for $Zn(Lap)_2(DMF)(H_2O)$ and $[M(Lap)_2]_n$ (M: Cd, Mn) complexes (Tables S1–3), full bond distances and angles (Tables S4–6), atomic anisotropic displacement parameters for the non-H atoms (Tables S7–9), and hydrogen atoms positions and their isotropic displacement parameters (Tables S10–12) are available from the authors upon request and have been deposited with the Cambridge Crystallographic Data Centre, under deposition numbers CCDC 1005149 (Zn), CCDC 1005150 (Cd) and CCDC 1005151 (Mn). Supplementary data associated with this article can be found, in the online version, at http://dx.doi.org/10.1016/j.molstruc.2015.01.042.

References

[1] M.K. Rafiullah, M.M. Suleiman, Phytochemistry 50 (1999) 439.
[2] M.F. Oliveira, T.L.G. Lemos, M.C. de Mattos, T.A. Segundo, G.M.P. Santiago, R. Braz-Filho, Ann. Acad. Bras. Cienc. 74 (2002) 211.
[3] R. Hernández-Molina, I. Kalinina, P. Esparza, M. Sokolov, J. Gonzalez-Platas, A. Estévez-Braun, E. Pérez-Sacau, Polyhedron 26 (2007) 4860.
[4] T.A. Annan, C. Peppe, D.G. Tuck, Can. J. Chem. 68 (1990) 423.
[5] M.A. Martínez, M.C.L. de Jiménez, E.E. Castellano, O.E. Piro, P.J. Aymonino, J. Coord. Chem. 56 (2003) 803.
[6] M.A. Martínez, M.C.L. Jiménez, E.E. Castellano, O.E. Piro, P.J. Aymonino, J. Argent. Chem. Soc. 93 (2005) 183.
[7] R.A. Farfán, J.A. Espíndola, M.A. Martínez, O.E. Piro, P.J. Aymonino, J. Coord. Chem. 62 (2009) 3738.
[8] F. Caruso, M.A. Martínez, M. Rossi, A. Goldberg, M.E. Chacón Villalba, P.J. Aymonino, Inorg. Chem. 48 (2009) 3529.

[9] Enraf-Nonius, COLLECT, Nonius BV, Delft, The Netherlands, 1997–2000.
[10] Z. Otwinowski, W. Minor, Methods Enzymol. 276 (1997) 307.
[11] A.L. Spek, PLATON, A Multipurpose Crystallographic Tool, Utrecht University, Utrecht, The Netherlands, 1998.
[12] G.M. Sheldrick, Acta Crystallogr. A64 (2008) 112.
[13] L.J. Farrugia, J. Appl. Cryst. 30 (1997) 565.
[14] W. Kabsch, Acta Cryst. A32 (1976) 922.
[15] H.D. Flack, Acta Cryst. A39 (1983) 876.
[16] L. Pasteur, C. R. Acad. Sci. Paris 26 (1848) 535.
[17] L. Pasteur, Anal. Chim. Phys. 24 (1848) 442.
[18] H.D. Flack, Acta Cryst. A65 (2009) 371.
[19] J. Wang, J. Niu, J. Mol. Struct. 693 (2004) 187.
[20] E. Rodríguez Frias, Substitution Reactions of Steric Factors in Ammine Complexes of Transition Metals, PhD Thesis, University of Barcelona, 2001.
[21] R.C. Agarwal, B. Rashmi, R.L. Prasad, Inorg. Metal – Org. Chem. 14 (1984) 171.
[22] K. Nakamoto, Infrared and Raman Spectra of Inorganic and Coordination Compounds, Part B, fifth ed., John Wiley and Sons, New York, 1997.
[23] F.L.S. Bustamante, M.M.P. Silva, W.A. Alves, C.B. Pinheiro, J.A.L.C. Resende, M. Lanznaster, Polyhedron 42 (2012) 43.
[24] H. Rostkowska, M.J. Nowak, L. Lapinski, L. Adamowicz, Spectrochim. Acta 54A (1998) 1091.
[25] P. Khandagale, R. Chicate, S.B. Joshi, B.A. Kulkarni, J. Alloys Compd. 392 (2005) 112.
[26] R.T. Singh, I. Ogata, R.E. Moore, C.W.J. Chang, P.J. Scheuer, Tetrahedron 24 (1968) 6053.
[27] S. Da Guia Mello Portugal, J.O. Machuca Herrero, E.M. Brinn, Bull. Chem. Soc. Jpn. 70 (1997) 2071.